

The Effect of Lattice Geometry on Ionic Transport in Lithium Garnets: Lattice-Gas Monte Carlo Simulations

Benjamin J. Morgan¹

¹*Department of Chemistry, University of Bath, Claverton Down, Bath, BA2 7AY*

(Dated: January 3, 2017)

=> ABSTRACT

I. INTRODUCTION

Solid electrolytes are distinguished from other materials by their capacity for ionic transport in the solid state. This property makes them useful in technologies such as solid-oxide fuel cells and all-solid-state lithium-ion batteries. In both cases, a solid electrolyte's utility critically depends its ionic conductivity, which quantifies the capacity for ion mobility to effect charge transport.

Solid electrolytes can be conceptually regarded as comprising two distinct sets of ions: those that are “mobile” and can travel multiple lattice spacings over experimentally relevant timescales, and those that are “fixed” and vibrate about their crystallographic sites. The set of fixed ions defines a three-dimensional network of diffusion pathways through which the mobile ions diffuse. The geometry of these diffusion paths is defined by the crystal structure, and represents one of the important differences between families of structurally-related solid electrolytes.

Developing high-conductivity solid electrolytes requires understanding how stoichiometry and structure affect ion transport. At a macroscopic scale, mass and charge transport are characterised by diffusion coefficients and ionic conductivities, respectively. These transport coefficients describe the long-time behaviour of ions, and represent ensemble averages over all microscopic diffusion processes undergone by individual mobile ions. A quantitative understanding of ionic conductivity across different solid electrolytes depends on the resolving the relationship between these microscopic diffusion processes and macroscopic transport coefficients.

In many solid electrolytes the microscopic transport of ions can be considered a sequence of discrete “hops”, where ions move between well-defined lattice sites.¹ If these hops are independent, every ion follows a random walk. The tracer diffusion coefficient, D^* and d.c. ionic conductivity, σ , can then be expressed as functions of the average hop rate per atom, $\tilde{\nu}$,² via^{3,4}

$$D^* = \frac{1}{6} a^2 \tilde{\nu}; \quad (1)$$

$$\sigma = \frac{Cq^2}{kT} \frac{1}{6} a^2 \tilde{\nu}; \quad (2)$$

where a is a characteristic hop distance, C is the charge carrier concentration, and q is the charge of the mobile ions. Combining equations 1 and 2 produces the “Nernst-

Einstein relation” between D^* and σ :

$$\frac{\sigma}{D^*} = \frac{Cq^2}{kT}. \quad (3)$$

These three equations provide quantitative relationships between the hop-rate, $\tilde{\nu}$, tracer diffusion coefficient, D^* , and ionic conductivity, σ . Their derivation, however, depends on all hops being independent—an assumption that holds only in the limit of very low carrier concentrations, or when the mobile ions are completely non-interacting.⁵

Practical solid electrolytes typically have high carrier concentrations, and interparticle interactions can be significant. In these cases, individual hop probabilities depend on the specific arrangement of nearby ions, and hops are no longer statistically independent. Instead, ion trajectories are “correlated”, and deviate from the random walk behaviour of non-interacting systems.^{3,6–8} Correlations between hops made by individual ions affect the relationship between average hop rate, $\tilde{\nu}$, and tracer diffusion coefficient, D^* , which becomes

$$D^* = \frac{1}{6} a^2 \tilde{\nu} f, \quad (4)$$

where f is a correlation factor that accounts for the deviations from random walk behaviour. Correlations between hops made by *different* ions affect the relationship between $\tilde{\nu}$ and σ , which becomes

$$\sigma = \frac{Cq^2}{kT} \frac{1}{6} a^2 \tilde{\nu} f_1, \quad (5)$$

where f_1 is the “collective” correlation factor. The relationship between σ and D^* is now

$$\frac{\sigma}{D^*} = \frac{Cq^2}{kT} \frac{f_1}{f}. \quad (6)$$

which differs from Nernst-Einstein behaviour (Eqn. 3) by the ratio of correlation factors $\frac{f_1}{f}$, commonly denoted as inverse of the Haven ratio, $H_R = \frac{f}{f_1}$.^{5,9} => this is clumsy writing at the moment

Quantitative relationships between microscopic hopping rates and macroscopic transport coefficients can, in principle, be obtained by combining experimental data for $\tilde{\nu}$, D^* , and σ . Ion hopping rates may be measured from NMR or muon spin-relaxation experiments,^{10–15} diffusion coefficients obtained from tracer diffusion

experiments,¹⁶ and ionic conductivities derived via impedance spectroscopy.^{17,18} Computational methods provide an increasingly used alternative to direct experimental studies. First principles calculations of barrier heights and vibrational partition functions along diffusion pathways give hopping rates.^{19,20} Molecular dynamics simulations can be used to directly calculate tracer diffusion coefficients and ionic conductivities.²¹ Often, however, it is convenient, or necessary, to use one member of $\{\tilde{\nu}, D^*, \sigma\}$ to calculate the others. All three parameters might not be known under equivalent experimental conditions, or one wishes to compare results from complementary approaches. Because the quantitative relationships between $\{\tilde{\nu}, D^*, \sigma\}$ depend on f and f_I (and their ratio H_R), it is important to know these correlation factors for the materials under consideration.

For many simple crystal lattices the correlation parameters $\{f, f_I, H_R\}$ have been calculated.^{5,22} For more complex crystal structures, however, these parameters are unknown. It is therefore common for studies to use the simplified Eqns. 1, 2, 3 to convert between $\{\tilde{\nu}, D^*, \sigma\}$. [INCORRECT “MODIFIED” NE EQUATION IN^{23,24}] This is equivalent to assuming non-interacting behaviour, where $f = 1, f_I = 1, H_R = 1$ and can introduce quantitative errors for materials where correlations are significant.

One example of technologically relevant solid electrolytes for which correlation effects are thought to be significant are the so-called lithium garnets. These are a family of solid lithium-ion electrolytes with composition $\text{Li}_x\text{M}_3\text{M}'_2\text{O}_{12}$,^{25,26} which have attracted significant attention as candidates for all-solid-state lithium-ion batteries, due to their high lithium-ion conductivities and broad electrochemical stability windows.²⁷

The garnet crystal structure provides an unusual three-dimensional network of lithium diffusion pathways, consisting of interlocking rings.²⁸ Each ring comprises 12 alternating tetrahedral and octahedral sites, with the tetrahedral sites acting as nodal points connecting adjacent rings (Fig. 1). Aliovalent substitution of the M and M' cations allows the lithium stoichiometry to be tuned across a broad range. A lithium stoichiometry of $x_{\text{Li}} = 9$ corresponds to a fully occupied lithium-site lattice, and research has focussed on “lithium stuffed” garnets, typically with $x_{\text{Li}} = 5 \rightarrow 7$. Ionic conductivities vary enormously as a function of x_{Li} , with σ increasing by $\sim 10^9$ between $\text{Li}_3\text{Ln}_3\text{Te}_2\text{O}_{12}$ and $\text{Li}_{6.55}\text{La}_3\text{Zr}_2\text{O}_{12}$,^{26,27} and it remains an open question precisely how the lithium diffusion coefficient and ionic conductivity vary with lithium stoichiometry. Resolving this is critical for the optimisation of ionic conductivity for this family of materials.

Theoretical considerations and published data indicate that lithium distribution and transport in lithium garnets exhibit significant correlation effects. The relationship between lithium stoichiometry and lithium transport coefficients is therefore expected to be non-ideal. Low coordination numbers for the lithium lattice-sites: 4 for tetrahedra and 2 for octahedra; suggest significant

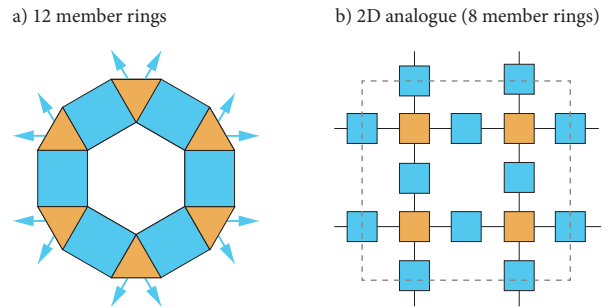


FIG. 1. Schematic of the ring structures that constitute the garnet lithium-diffusion network. a) Each ring consists of 12 alternating tetrahedra (orange) and octahedra (blue). Arrows show connections to neighbouring rings.²⁸ b) A 2D analogue of interconnected 8-membered rings of alternating “tetrahedra” and “octahedra”.

site-blocking effects.²⁸ Short distances of ~ 2.4 Å between lithium sites suggest strong Li–Li Coulomb repulsion, becoming increasingly significant at high Li content.^{29–32} The presence of two non-equivalent sets of lattice sites is a further factor: if ideally distributed, lithium ions would occupy the octahedral and tetrahedral lattice sites in a 2:1 ratio at all Li concentrations. Neutron data however show that at low lithium content ($x_{\text{Li}} = 3$) only tetrahedral sites are occupied,³³ while at higher lithium content ($x_{\text{Li}} = 5 \rightarrow 7$) octahedral sites become preferentially occupied.^{26,31} Experimental conductivities have also been found to show non-linear dependence on x_{Li} ,³⁴ and to deviate strongly from ideal values predicted (via Eqn. 2) from muon-spin-spectroscopy hopping rates.¹⁴ Further evidence for correlated transport in lithium garnets has been provided by computational studies. Molecular dynamics simulations have been used to identify a variety of correlated diffusion processes,^{24,35–37} while calculated diffusion coefficients and ionic conductivities show non-Nernst-Einstein behaviour ($H_R < 1$).^{38,39} The quantitative effects of correlation in lithium garnets, however, are not known, and conversions between hop rates, diffusion coefficients, and ionic conductivities are often approximated by assuming uncorrelated motion.^{14,15,17,35,40–48}

To quantitatively describe the relationship between lithium stoichiometry and ionic conductivity in lithium-ion garnets, it is essential to consider non-ideal distributions and transport of the lithium ions. Here we present a computational analysis of these issues, using lattice-gas kinetic Monte Carlo simulations of diffusion on a “garnet” lattice, for a range of model Hamiltonians. We calculate f and f_I as functions of carrier concentration (Li stoichiometry), first for a non-interacting [NEED TO BE CONSISTENT WITH TERMINOLOGY. VOLUME-EXCLUSION IS “NON-INTERACTING” IN THE SENSE THAT THERE ARE NO INTERACTION ENERGIES BETWEEN PARTICLES TO CONSIDER, WHICH IS EQUIVALENT TO THE SYSTEM ENERGY BEING EQUAL FOR ALL ACCESSIBLE

CONFIGURATIONS OF PARTICLES WITHIN THE LATTICE] / volume-exclusion-only model, and then for models that include on-site single-particle energies and/or nearest-neighbour repulsion interactions. In addition to self- and collective-correlation factors, we present site occupation populations, diffusion coefficients, and effective ionic conductivities for this range of simulation models, allowing us to discuss how different interactions contribute to non-ideal behaviour, and modify the relationships between particle hopping rate, diffusion coefficient, and ionic conductivity.

=> We find that ... [do we want to include a brief summary of results here?] => edit / delete / revise the rest of this section →

II. METHODS

Lattice-gas Monte Carlo simulations describe the diffusion of a set of mobile ions populating some host lattice, expressed as a graph of interconnected sites. Every lattice site is either occupied or vacant, and during a simulation the mobile ions undergo a sequence of hops from site to site. These hops are randomly selected, with relative probabilities that satisfy the principle of detailed balance and represent the underlying model Hamiltonian. The simplest model considered here is a “non-interacting” volume-exclusion-only model.⁴⁹ Double occupancy of sites is forbidden, and allowed hops are all equally likely. Non-interacting models allow the pure geometric effect of the lattice to be evaluated, but neglect other interactions that may be significant in corresponding experimental systems. For the garnet lattice, here we also consider the effect of nearest-neighbour interactions between mobile ions, described by a nearest-neighbour repulsion energy, E_{nn} , and interactions between single ions and the lattice, described by on-site energies for tetrahedral versus octahedral sites, E_T , E_O . The energy of any configuration of occupied sites, j is given by

$$E = \sum_j n_j^{nn} E_{nn} + E_{site}^j, \quad (7)$$

where n_j^{nn} is the number of occupied nearest neighbour sites for (occupied) site j . For interacting systems, the relative probability of hop i depends on the change in total energy ΔE_i for the system if this hop was selected:

$$P_i \propto \begin{cases} \exp\left(\frac{\Delta E_i}{kT}\right), & \text{if } \Delta E_i > 0 \\ 1, & \text{otherwise.} \end{cases} \quad (8)$$

For our interacting systems, the change in energy for each candidate hop can depend on the change in number of nearest-neighbour interactions and the change in on-site energy for moving from a tetrahedral to octahedral site (or vice versa):

$$\Delta E_i = \Delta n_{nn} E_{nn} + \Delta E_{site}. \quad (9)$$

At each simulation step, one hop is randomly selected according to the set of relative probabilities. The corresponding ion is moved, and a new set of relative hop probabilities is generated for the subsequent step.

In the limit of a large number of hops, the tracer- and collective-correlation factors can be evaluated as

$$f = \frac{\sum_i \langle R^2 \rangle}{Na^2}, \quad (10)$$

where $\langle R^2 \rangle$ is the mean-squared displacement of the mobile ions, and N is the total number of hops during the simulation, and

$$f_1 = \frac{|\sum_i R_i|^2}{Na^2}, \quad (11)$$

where $\sum_i R_i$ is the *net* displacement of all mobile particles. In both cases the denominators correspond to the limiting behaviour for uncorrelated diffusion.

To allow time-dependent properties to be evaluated, we perform our lattice-gas Monte Carlo simulations within a rejection-free kinetic Monte Carlo scheme. For each simulation step, k , the set of hop probabilities, $\{P_{i,k}\}$, are converted to rates, $\{\Gamma_{i,k}\}$ by scaling by a common prefactor of 10^{13} s^{-1} . After selecting a hop, the simulation time is updated by $\Delta t = Q_k^{-1} \ln(1/u)$, where Q_k is the “total rate”; $Q_k = \sum_i \Gamma_{i,k}$, and u is a uniform random number $u \in (0, 1]$. This approach provides time-averaged site occupations, and directly calculated diffusion coefficients and ionic conductivities.

Our lattice-gas kinetic Monte Carlo simulations were performed using the `lattice.mc` code.⁵⁰ Simulations were performed for an ideal cubic $2 \times 2 \times 2$ garnet lattice, with 384 octahedral sites and 192 tetrahedral sites. The lattice site coordinates were generated from the cubic high-temperature $\text{Li}_7\text{La}_3\text{Zr}_2\text{O}_{12}$ (LLZO) structure (ICSD #422259),²⁸ with the centres of octahedra and tetrahedra defined by the oxygen sub-lattice used to define the corresponding site coordinates. In cubic LLZO, each lithium-octahedron contains a “split” pair of distorted $96h$ sites, separated by 0.81 Å. The construction used here considers each octahedron as a single ideal $48g$ site. The network of diffusion pathways includes connections between nearest-neighbour sites only, i.e. all connections are between neighbouring tetrahedral–octahedral pairs. **[CALCULATED DIFFUSION COEFFICIENTS ARE PRESENTLY IN $\text{bohr}^2 \text{ s}^{-1}$.]** For each simulation, n_{Li} mobile ions are randomly distributed across the lattice sites. 1000 equilibration steps are performed before 10,000 production steps.

For each set of model parameters, $\{E_{nn}, \Delta E_{site}\}$, simulations were performed across the full range of possible lithium stoichiometry ($x_{\text{Li}} = 9$ corresponds to $n_{\text{Li}} = 576$). For each system, data were collected as an average over 5000 trajectories.

=> Minimal documentation for this code. Push to github + documentation + docstrings + doi

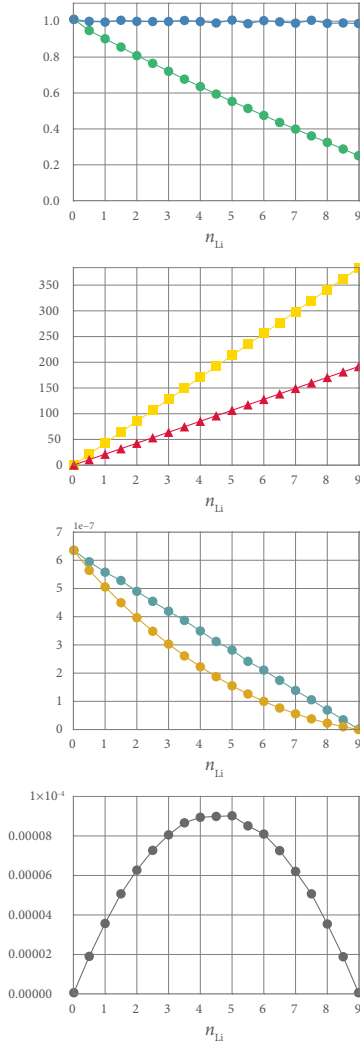


FIG. 2. CAPTION a) TODO, b) TODO, c) TODO, d) TODO.

III. RESULTS

A. Non-Interacting Particles and Geometric Effects

We first examine the pure geometric effect of the garnet lattice by modelling non-interacting systems, for which deviations from random walk behaviour emerge purely from volume exclusion effects. Fig. 2 shows the calculated self- and collective-correlation factors, f and f_I , average tetrahedral and octahedral site occupations, n_{tet} and n_{oct} , tracer and “jump” diffusion coefficients, D^* and D_J , and effective (reduced) ionic conductivity, σ' , for the volume-exclusion-only simulations, as a function of x_{Li} .

In the single particle limit, $x_{\text{Li}} \rightarrow 0$, there are no blocking effects, and particles follow a random walk. With increasing concentration of mobile ions, however, single particle diffusion increasingly deviates from random walk behaviour. The tracer correlation factor, f , decreases

from $f = 1$ in the single particle limit $x_{\text{Li}} \rightarrow 0$ to $f = 0.25$ in the single vacancy limit $x_{\text{Li}} \rightarrow 9$, with approximately linear dependence on x_{Li} ⁵¹.

The magnitude of the tracer correlation effect for different lattice geometries can be characterised by considering f in the limit of a single vacancy, f_v . For the garnet lattice this is the limit $x_{\text{Li}} \rightarrow 9$. Table I presents f_v values previously calculated for common 3D lattices,⁵² and for a 1D chain,⁵³ alongside our value for the garnet lattice. For the garnet lattice, $f_v = 0.25$. This is smaller than for all of the other 3D lattices, by at least a factor of 2, corresponding to unusually strong correlation effects. This result can be understood as a consequence of the particular garnet lattice geometry. For a general set of 3D lattices, as the number of nearest neighbours of each lattice site, z , decreases, f_v also decreases, and correlation effects become more significant. The garnet lattice has both 4-coordinate (tetrahedral) and 2-coordinate (octahedral) sites, and long ranged diffusion follows an alternating T→O→T→O pattern. The calculated value of $f_v = 0.25$ is halfway between the values for the 4-coordinate diamond lattice ($f_v = 0.5$) and for a 1-D chain, where every site is 2-coordinate ($f_v = 0$). This suggests that the extreme low value of f_v for the garnet lattice is a consequence of the low coordination of the lattice sites, in particular the local 1D coordination at the octahedral sites, which act as bottlenecks for long-ranged diffusion.

Lattice	z	f_v
Face centered cubic ⁵²	12	0.78146
Body centred cubic ⁵²	8	0.72722
Simple cubic ⁵²	6	0.65311
Diamond ⁵²	4	0.5
Garnet [This work]	[4+2]	0.25
1D chain ⁵³	2	0.0

TABLE I. Vacancy correlation factors for some common crystal lattices. z is the number of nearest neighbours for each site in the lattice.

For any non-interacting system, the hops made by different particles are uncorrelated, and $f_I = 1$ for all x_{Li} , making $H_R = f$. There are also no correlations between site occupations, and the mobile particles are randomly distributed over the available octahedral and tetrahedral sites, with a 2:1 population ratio that reflects the underlying lattice geometry.

We also consider three measures of ionic transport in this system.⁵⁴ Fig. 2(c) shows the tracer diffusion coefficient, D^* (Eqn. 4) and the “jump diffusion coefficient”, D_J ⁵⁵, calculated as

$$D_J = \frac{|\sum_i R_i|^2}{6Nt}. \quad (12)$$

At a fixed temperature D_J is proportional to the mobility, and measures the ease with which the mobile particles undergo collective migration. Both D^* and D_J decrease

monotonically from $x_{\text{Li}} = 0$ to $x_{\text{Li}} = 9$ ($x = 0 \rightarrow 1$), as the number of vacancies available for mobile particles to hop to decreases. For the non-interacting system there are no correlations between hops made by different particles, and the jump diffusion coefficient is proportional to $(1 - x)$.^{49,55} [THIS IS NOW x WITH A MAXIMUM OF 1, I.E. CONCENTRATION]. The tracer diffusion coefficient, however, shows the effect of correlations between hops made by individual particles, and varies according to $D^* \propto (1 - x)f$. The ionic conductivity of a system depends on both the charge-carrier concentration, and the ionic mobility (which is proportional to D_J). To examine the relationship between carrier concentration and *relative* ionic conductivities, we also can consider a “reduced” conductivity, σ' ,⁵⁶ given by

$$\sigma' = xD_J. \quad (13)$$

For any non-interacting system, $\sigma' \propto x(1 - x)$, with a maximum at $x = 0.5$ (Fig. 2(d)).

B. Interacting Particles

The conceptual simplicity of the non-interacting system makes it a convenient starting point for understanding the factors affecting ionic transport in different lattices. In real Li-garnet materials, however, interactions between lithium ions, or between lithium ions and the host lattice, can be significant. Lithium ions carry positive charge, and can be expected to experience mutual Coulomb repulsion, and the different oxygen-coordination environments of octahedral and tetrahedral sites can be expected to produce a preference for occupation by lithium at one site versus the other. Within the lattice-gas Monte Carlo scheme, we consider these two factors by introducing, first, nearest-neighbour repulsion, and second, an octahedral versus tetrahedral site preference.

[MOVE THIS COMMENT TO THE INTRODUCTION OR/AND THE DISCUSSION?: SIMULATIONS OF OTHER LATTICE GEOMETRIES WHERE NEAREST-NEIGHBOUR REPULSION HAS BEEN MODELLED PREDICT PARTICLE ORDERING AT SPECIFIC LATTICE OCCUPATION FRACTIONS (DEPENDENT ON THE LATTICE GEOMETRY UNDER CONSIDERATION) AND IS ASSOCIATED WITH STRONG SELF- AND COLLECTIVE-CORRELATION EFFECTS.]

1. Nearest-Neighbour repulsion

To examine the effect of Li–Li repulsion, we consider a simplified model with only nearest-neighbour repulsion. The energy of Li at each specific site now depends on the number of occupied neighbouring sites and individual hop probabilities now depend on whether they increase or decrease the total number of nearest-neighbour pairs. Fig. => plot of f , f_1 , H_R , n_{tet} , n_{oct} , σ' . presents results of LGMC simulations performed for $E_{\text{nn}} = 0.0$ – 3.0 kT .

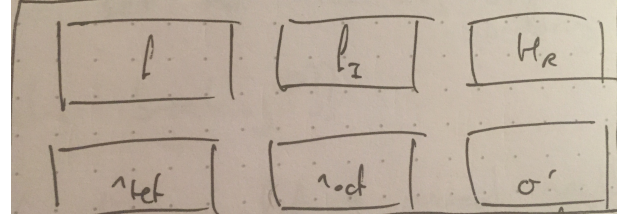


FIG. 3. CAPTION

Repulsive nearest-neighbour interactions disfavour simultaneous occupation of adjacent sites, and promote ordering of particles across alternating occupied–vacant–occupied–vacant sites. This ordering causes the single-particle correlation behaviour to deviate from that of the non-interacting system, and introduces collective correlations between the mobile ions. In a lattice with only one crystallographic site complete ordering would occur at half-site-occupancy, corresponding to $x_{\text{Li}} = 4.5$ for the garnet lattice. The behaviour of f and f_1 with increasing E_{nn} approximately follow this prediction. Both correlation factors have their non-interacting values in the empty and fully-occupied lattice limits $x \rightarrow 0, x \rightarrow 1$ and decrease at intermediate stoichiometries. Both correlation factors also show a strong decrease at $x_{\text{Li}} = 6$, and this is a consequence of the existence of two non-equivalent sites in the garnet lattice.

The garnet lattice consists of octahedral and tetrahedral sites in a 2:1 ratio, with corresponding site occupations for the non-interacting system (Fig. 2(b)). With non-zero nearest-neighbour repulsion, this preference for octahedral sites is reinforced by the preference for alternating occupied–unoccupied sites. Given that octahedral site occupation is entropically favoured, any non-dilute population of particles can minimise its energy by occupying *only* octahedral sites. This effect is strongest at two-thirds site occupation ($x_{\text{Li}} = 6$) where the octahedral sites are fully occupied and the tetrahedral sites are fully vacant. In this fully ordered system, correlation effects are maximised: any O→T hop by a single particle is likely to be quickly reversed, and diffusion is possible only for highly correlated collective movement by groups of particles³⁷. This effect is visible in the effective conductivity, σ' , which drops sharply at $x_{\text{Li}} = 6$.⁵⁷

[KOZINSKY *et al.* HAVE ALSO PROPOSED A FULLY ORDERED PHASE AT $x_{\text{Li}} = 6$, FROM FIRST-PRINCIPLES CALCULATIONS AND GROUP THEORY ANALYSIS, THAT DIFFERS FROM THE PURE OCTAHEDRAL OCCUPATION DESCRIBED HERE⁵⁸. THE FULLY-ORDERED CONFIGURATION OBSERVED HERE AT $x_{\text{Li}} = 6$ IS DIFFERENT FROM THAT PROPOSED BY KOZINSKY *et al.*⁵⁸. THAT WORK PREDICTED MIXED OCCUPATION OF OCTAHEDRAL AND TETRAHEDRAL SITES. IN THAT CASE CONNECTED TO SYMMETRY BREAKING / IN THIS CASE THE CUBIC LATTICE SYMMETRY IS MAINTAINED]

2. Site asymmetry

The non-interacting model, discussed above, assumes that mobile Li ions show an equal preference for octahedral and tetrahedral sites: the site “type” is only relevant in that it defines the connectivity of each site within the lattice graph. This symmetry in on-site energies means the populations of occupied octahedral and tetrahedral sites simply follow a 2:1 ratio. In experimental Li-garnet samples with $x(\text{Li}) = 3$, e.g. $\text{Li}_3\text{Y}_3\text{Te}_2\text{O}_{12}$, the lithium ions exclusively occupy the tetrahedral sites³³. This suggests that in the absence of other interactions, there is an energetic penalty for occupying octahedral rather than tetrahedral sites. We denote this energy cost $\Delta E_{\text{site}} = E_{\text{oct}} - E_{\text{tet}}$. In the following we describe LGMC simulations for otherwise non-interacting particles, with $\Delta E_{\text{site}} = 0 - 5kT$.

With increasing ΔE_{site} , tetrahedral sites are preferentially occupied with respect to octahedral sites: at higher values of ΔE_{site} all lithium ions preferentially occupy tetrahedral sites, with octahedral sites only occupied for $x_{\text{Li}} > 3$ when the tetrahedral sites are fully occupied. In the limit of $\Delta E_{\text{site}} \rightarrow \infty$ (equivalent to $T \rightarrow 0$) x_{Li} corresponds to an ordered arrangement with all the tetrahedral sites occupied and all the octahedral sites vacant. The preferential tetrahedral occupation and associated ordering correlates with an increased single particle correlation (decreased f) and introduces collective correlation across the full Li stoichiometry range, with the largest effect (smallest $f_m I$) at $x_{\text{Li}} = 3$. The result that the Li preferentially order for specific numbers of occupied sites, and that this is associated with strong single-particle and collective correlation effects is consistent with equivalent results obtained for other lattices for which the effect of alternating site energies have been modelled => e.g. refs and examples? 2D hexagonal lattice The Haven ratio, H_R , is slightly decreased relative to the non-interacting case for $x_{\text{Li}} < 3$, and approximately follows the non-interacting behaviour for $x_{\text{Li}} > 3$.

3. Combined site inequality and nearest-neighbour repulsion

In real Li-garnet materials, both site inequality and Li-Li repulsion can be expected to play a role. We have also performed simulations with both parameters. The low computational cost of LGMC simulations allows the $\{x_{\text{Li}}, \Delta E_{\text{site}}, E_{\text{nn}}\}$ parameter space to be mapped. The simulation data from these calculations are included in the SI / Appendix, and are available as a data set. => include example of both parameters varying, e.g. $\Delta E_{\text{site}} = 3.0\text{eV}$, $E_{\text{nn}} = 3.0\text{eV}$. Introduces “correlation” features at $x = 3, 6$.

Much research in Li-garnets concerns optimising the composition so that the ionic conductivity is maximised. Part of this is identifying the Li concentration that maximises the ionic conductivity of this family of materials. => who has proposed arguments for im-

proving ionic conductivity by tuning x_{Li} ?

$$\sigma_{\text{dc}} \propto c(1 - c) f_{\text{I}} \quad (14)$$

[IS THIS DISCUSSED BY ANYONE? CF. KUTNER⁴⁹ BEHAVIOUR IN NON-INTERACTING CASE IS DESCRIBED BY KUTNER. INTERACTIONS (BETWEEN PARTICLES OR WITH THE LATTICE) INTRODUCE AN ADDITIONAL SCALING f_{I} WHICH DESCRIBES THE EFFICIENCY WITH WHICH DIFFUSIVE JUMPS CONTRIBUTE TO COLLECTIVE TRANSPORT.] σ_{dc} is proportional to three terms: the => rewrite this in notation consistent with what appeared earlier The $c(1 - c)$ factor gives a parabolic dependence with a maximum ionic conductivity as $x = \frac{9}{2}$, as seen (above?) for the non-interacting / equivalent sites system. By “switching on” additional physics: on-site energies and interactions between mobile ions, $f_{\text{I}} \neq 1$, with f_{I} a function of the interaction strengths, the lattice topology, and the carrier concentration. The optimal x_{Li} for a given material therefore depends on the behaviour of $f_{\text{I}}(x_{\text{Li}})$.

The low computational cost of the LGMC simulations have allowed us to calculate an effective ionic conductivity σ' as a function of $\{x_{\text{Li}}, \Delta E_{\text{site}}, E_{\text{nn}}\}$. Considering this data set, we can pose the following question: what is the value of x_{Li} that maximises the (effective) ionic conductivity, at each combination of $\Delta E_{\text{site}}, E_{\text{nn}}$

At any combination of $\Delta E_{\text{site}}, E_{\text{nn}}$ we can identify the x_{Li} that gives the maximum ionic conductivity, and then map how $\arg \max \sigma'(x_{\text{Li}})$ depends on the scale of interactions. This defines a surface in model parameter space, which is shown as a contour plot in Fig. 5. A wide range of “optimal” x_{Li} values are identified. With regard to real materials, the question is then, which regions of parameter space correspond to real materials, and to what degree the simple parameters considered here vary across possible chemistries of the garnet family. For example => discussion of effect of cation size / polarizabilities on conductivity trends? Larger cations: larger lattice parameter \rightarrow decreased nearest-neighbour repulsion? Possibly modify balance of ΔE_{sites} ? High polarisability? \rightarrow increased screening? and reduced E_{nn} ? Poses an interesting challenge: to what degree can effective parameters describing a simplified Hamiltonian (such as those employed here) be extracted from e.g. electronic structure calculations on real garnet materials?

IV. DISCUSSION

Summary. What was the motivation (A \rightarrow B). What have we done to explore / solve this problem? What are notable results?

Summary \rightarrow How well does this meet the goals laid out in the introduction?

=> To add above: nearest-neighbour interactions and relative site energies are possibly manipulated through the choice of lattice cations, because this determines

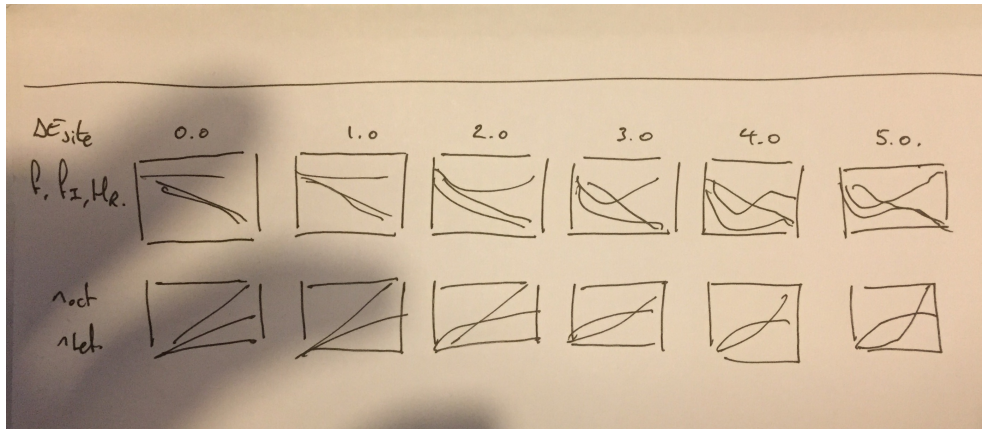


FIG. 4. CAPTION

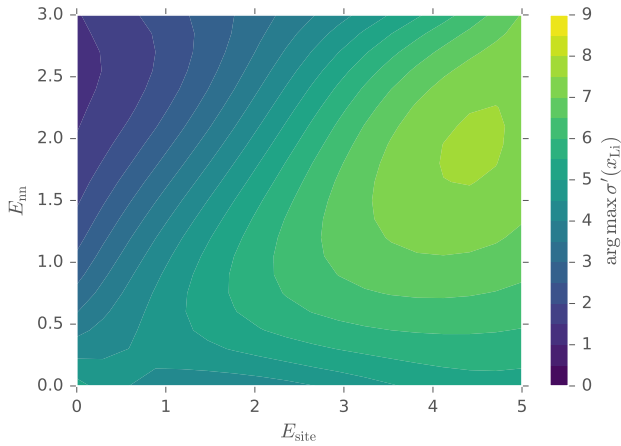


FIG. 5. CAPTION

lattice-site separations, and also the dielectric screening between adjacent Li ions.

Discuss the benefits / problems with this kind of model Hamiltonian analysis (speed / sampling of parameter space / direct interpretation of simple conceptual interactions) Shortcomings: barrierless kMC (all barriers could

be quantified, but is there a straightforward way to map across interactions away from “known” materials? => cite relevant VdV / Ceder papers discussing e.g. variation in barriers with composition)

Other issues: assumption of a perfect lattice? (cf. Kozinsky / t-LLZO) Only single particle jumps (again t-LLZO shown to have many-particle jumps³⁷ also Sci. Rep. paper if published?)

Additional comment (re: Lucy) can invert this question: experimental data on maximum σ can be used to (qualitatively) estimate relative interaction energies by identifying model parameters that “best fit” experimental data for specific materials.

V. ACKNOWLEDGEMENTS

B. J. M. acknowledges support from the Royal Society (UF130329). B. J. M. would also like to thank M. Burbano, M. Salanne, and S. Adams for stimulating discussions.

VI. SUPPLEMENTARY INFORMATION

=> figures showing simulation data for combined $\Delta E_{\text{site}}, E_{\text{nn}}$ systems.

¹ Describing ionic transport as sequences of discrete hops breaks down for “super-ionic” solid electrolytes, with extremely mobile ions. The set of criteria for considering ionic transport to operate in a particle hopping regime are discussed by Catlow in C. R. A. Catlow, Sol. Stat. Ionics **8**, 89 (1983).

² The average hop rate per atom is the inverse of the mean residence time, $\tilde{\nu} = 1/\tilde{\tau}$. The contribution from each atom is a sum over individual hop rates, Γ_i , and is therefore related to the “total rate” of the kMC method via $\tilde{\nu} = \langle Q \rangle / N$.⁵³

³ R. E. Howard and A. B. Lidiard, Rep Prog Phys. **27**, 161 (1964).

⁴ A. M. Stoneham, ed., *Ionic Solids at High Temperatures* (World Scientific, 1989).

⁵ G. E. Murch, Sol. Stat. Ionics **7**, 177 (1982).

⁶ J. Bardeen and C. Herring, *Imperfections in Nearly Perfect Crystals* (John Wiley & Sons, Inc., 1952).

⁷ K. Compagnon and Y. Haven, Trans. Faraday Soc. **54**, 1498 (1958).

⁸ A. R. Allnatt and A. B. Lidiard, *Atomic Transport in Solids* (Cambridge University Press, 2008).

⁹ S. A. Akbar, J. Appl. Phys. **75**, 2851 (1994).

¹⁰ M. Wilkening, W. Kuchler, and P. Heitjans, Phys. Rev. Lett. **97**, 065901 (2006).

- ¹¹ B. Ruprecht, M. Wilkening, R. Uecker, and P. Heitjans, *Phys. Chem. Chem. Phys.* **14**, 11974 (2012).
- ¹² L. Enciso-Maldonado, M. S. Dyer, M. D. Jones, M. Li, J. L. Payne, M. J. Pitcher, M. K. Omir, J. B. Claridge, F. Blanc, and M. J. Rosseinsky, *Chem. Mater.* **27**, 2074 (2015).
- ¹³ A. B. Santibáñez-Mendieta, C. Didier, K. K. Inglis, A. J. Corkett, M. J. Pitcher, M. Zanella, J. F. Shin, L. M. Daniels, A. Rakhmatullin, M. Li, M. S. Dyer, J. B. Claridge, F. Blanc, and M. J. Rosseinsky, *Chem. Mater.* **28**, 7833 (2016).
- ¹⁴ H. Nozaki, M. Harada, S. Ohta, I. Watanabe, Y. Miyake, Y. Ikeda, N. H. Jalarvo, E. Mamontov, and J. Sugiyama, *Sol. Stat. Ionics* **262**, 585 (2014).
- ¹⁵ M. Amores, T. E. Ashton, P. J. Baker, E. J. Cussen, and S. A. Corr, *J. Mater. Chem. A* **4**, 1729 (2016).
- ¹⁶ R. D. Bayliss, S. N. Cook, S. Kotsantonis, R. J. Chater, and J. A. Kilner, *Adv. Energy Mater.* **4**, 1 (2014).
- ¹⁷ W. G. Zeier, S. Zhou, B. Lopez-Bermudez, K. Page, and B. C. Melot, *ACS Appl. Mater. Int.* **6**, 10900 (2014).
- ¹⁸ B. Lopez-Bermudez, W. G. Zeier, S. Zhou, A. J. Lehner, J. Hu, D. O. Scanlon, B. J. Morgan, and B. C. Melot, *J. Mater. Chem. A* **4**, 6972 (2016).
- ¹⁹ A. Van der Ven, G. Ceder, M. Asta, and P. Tepesch, *Phys. Rev. Lett.* **64**, 184307 (2001).
- ²⁰ M. Mantina, Y. Wang, R. Arroyave, L. Q. Chen, Z. K. Liu, and C. Wolverton, *Phys. Rev. Lett.* **100**, 215901 (2008).
- ²¹ B. J. Morgan and P. A. Madden, *J. Phys-Condens. Matter* **24**, 275303 (2012).
- ²² R. J. Friauf, *J. Appl. Phys.* **33**, 494 (1962).
- ²³ Y. Wang, M. Klenk, K. Page, and W. Lai, *Chem. Mater.* **26**, 5613 (2014).
- ²⁴ M. Klenk and W. Lai, *Phys. Chem. Chem. Phys.* , 8758 (2015).
- ²⁵ V. Thangadurai, H. Kaack, and W. Weppner, *J. Am. Ceram. Soc.* **86**, 437 (2003).
- ²⁶ V. Thangadurai, D. Pinzaru, S. Narayanan, and A. K. Baral, *J. Phys. Chem. Lett.* **6**, 292 (2015).
- ²⁷ J. C. Bachman, S. Muy, A. Grimaud, H.-H. Chang, N. Pour, S. F. Lux, O. Paschos, F. Maglia, S. Lupart, P. Lamp, L. Giordano, and Y. Shao-Horn, *Chem. Rev.* **116**, 140 (2016).
- ²⁸ J. Awaka, A. Takashima, K. Kataoka, N. Kijima, Y. Idemoto, and J. Akimoto, *Chem. Lett.* **40**, 60 (2011).
- ²⁹ M. P. O’Callaghan and E. J. Cussen, *Chem. Comm.* , 2048 (2007).
- ³⁰ M. P. O’Callaghan and E. J. Cussen, *Sol. Stat. Sci* **10**, 390 (2008).
- ³¹ E. J. Cussen, *J. Mater. Chem.* **20**, 5167 (2010).
- ³² Y. Wang, A. Huq, and W. Lai, *Sol. Stat. Ionics* **255**, 39 (2014).
- ³³ M. P. O’Callaghan, D. R. Lynham, E. J. Cussen, and G. Z. Chen, *Chem. Mater.* **18**, 4681 (2006).
- ³⁴ T. Thompson, A. Sharafi, and M. D. Johannes, *Adv. Energy Mater.* (2015).
- ³⁵ R. Jalem, Y. Yamamoto, H. Shiiba, M. Nakayama, H. Munakata, T. Kasuga, and K. Kanamura, *Chem. Mater.* **25**, 425 (2013).
- ³⁶ K. Meier, T. Laino, and A. Curioni, *J. Phys. Chem. C* (2014).
- ³⁷ M. Burbano, D. Carlier, F. Boucher, B. J. Morgan, and M. Salanne, *Phys. Rev. Lett.* **116**, 135901 (2016).
- ³⁸ M. J. Klenk and W. Lai, *Sol. Stat. Ionics* **289**, 143 (2016).
- ³⁹ M. Burbano, B. J. Morgan, and M. Salanne, “Li garnet md paper,” In Preparation.
- ⁴⁰ A. Kuhn, S. Narayanan, L. Spencer, G. Goward, V. Thangadurai, and M. Wilkening, *Phys. Rev. B* **83**, 094302 (2011).
- ⁴¹ A. Kuhn, V. Epp, G. Schmidt, S. Narayanan, V. Thangadurai, and M. Wilkening, *J. Phys-Condens. Mat* **24**, 035901 (2011).
- ⁴² L. J. Miara, S. P. Ong, Y. Mo, W. D. Richards, Y. Park, J. M. Lee, H.-S. Lee, and G. Ceder, *Chem. Mater.* **25**, 3048 (2013).
- ⁴³ J. R. Rustad, arXiv (2016), related:H1H1zFMCzesJ.
- ⁴⁴ W. Gu, M. Ezbiri, R. P. Rao, M. Avdeev, and S. Adams, *Sol. Stat. Ionics* **274**, 100 (2015).
- ⁴⁵ S. Adams and P. P. Rao, *J. Mater. Chem.* **22**, 1426 (2012).
- ⁴⁶ A. Düvel, A. Kuhn, L. Robben, M. Wilkening, and P. Heitjans, *J. Phys. Chem. C* **116**, 15192 (2012).
- ⁴⁷ S. Narayanan, V. Epp, M. Wilkening, and V. Thangadurai, *RSC Adv.* **2**, 2553 (2012).
- ⁴⁸ A. Ramzy and V. Thangadurai, *ACS Appl. Mater. Int.* **2**, 385 (2010).
- ⁴⁹ R. Kutner, *Phys. Lett.* **81A**, 239 (1981).
- ⁵⁰ B. J. Morgan, “*lattice_mc*,”.
- ⁵¹ A linear least-squares fit to these data gives $R^2 = 0.9974$.
- ⁵² K. Compaan and Y. Haven, *Trans. Faraday Soc.* **52**, 786 (1956).
- ⁵³ H. Mehrer (Springer, 2007).
- ⁵⁴ Because the lattice-gas model used here considers hops as barrierless, where hopping probabilities only depend on energy differences between initial and final states, the effective transport coefficients calculated here cannot be directly compared to experimental values. Introducing fixed barrier heights for tet \leftrightarrow oct hops is equivalent to scaling the hopping prefactor $\tilde{\nu}$, which preserves *relative* differences in the transport coefficients presented here. A more realistic model would need to account for the influence of local site occupations on individual hopping barriers, see e.g. Ref.⁵⁹, and would give quantitative deviations from the trends presented here.
- ⁵⁵ A. Van der Ven, J. Bhattacharya, and A. A. Belak, *Acc. Chem. Res.* **46**, 1216 (2013).
- ⁵⁶ For a system with a single mobile species, the reduced conductivity is equal to the true ionic conductivity if $\frac{VkT}{q^2} = 1$.
- ⁵⁷ Kozinsky *et al.* have also proposed a fully ordered phase at $x_{Li} = 6$, from a combined first-principles calculations and group theory analysis⁵⁸. Their proposed ground state differs from the pure octahedral occupation predicted here, and consists of mixed octahedral and tetrahedral occupation.
- ⁵⁸ B. Kozinsky, S. A. Akhade, P. Hirel, A. Hashibon, C. Elsässer, P. Mehta, A. Logéat, and U. Eisele, *Phys. Rev. Lett.* **116**, 055901 (2016).
- ⁵⁹ A. Van Der Ven and G. Ceder, in *Handbook of Materials Modelling* (2010) pp. 1–28.